Journal of Catalysis **193,** 238–247 (2000)
doi:10.1006/jcat.2000.2894, available online at http://www.idealibrary.com on IDEAL®

Influence of the Degree of Carburization on the Density of Sites and Hydrogenating Activity of Molybdenum Carbides

Jae-Soon Choi, Guy Bugli, and Gérald Djéga-Mariadassou[1]

Laboratoire Réactivité de Surface, Université Pierre et Marie Curie, CNRS-UMR 7609, Casier 178, 4 Place Jussieu, 75252 Paris Cedex 05, France

Received December 1, 1999; revised April 17, 2000; accepted April 17, 2000

Temperature-programmed carburization of molybdic acid with CH_4/H_2 mixtures led to hexagonal Mo_2C with specific surface areas ranging from 40 to 91 $m^2\ g^{-1}$. The carburization was found to go through Mo_4O_{11}, MoO_2, and Mo metal. Whatever was the parameter of carburization, no significant change of the lattice parameters of Mo_2C was detected by XRD. The primary particles of the resulting carbides were found to be single crystals. Elemental analysis evidenced different bulk carbon contents of carbides depending on the conditions of synthesis. Nevertheless, this kind of analysis only gives global data to monitor the completion of carburization. Without free carbon contamination, all accessible Mo atoms were able to chemisorb oxygen. So oxygen chemisorption was proposed as a molecular probe to control the free carbon deposition. Counting of noble metal-like sites was possible by selective CO chemisorption, which was found to selectively deactivate active sites in benzene hydrogenation. CO titrated from 3 to 58% of a monolayer of surface Mo atoms. This evolution of the density of sites titrated by CO was interpreted in terms of the "degree of carburization" of materials linked to both surface carbidic carbon and residual oxygen contents as evidenced by TPR measurements of Mo_2C prepared *in situ*. The evaluation of the quality of each Mo site titrated by CO was done by benzene hydrogenation at room temperature. The carbides were found to be as active as Ru/Al_2O_3. A significant increase of the activity per site was observed on Mo_2C, when the density of sites titrated by CO was increased. It means that the degree of carburization affects not only the number of active sites, but also the quality of these sites. These results are in good agreement with the general concept speculated on the noble metal-like behavior of Mo_2C: the higher the carbidic carbon content and the lower the residual oxygen content in Mo lattice, the higher will be the noble metal-like behavior.

Key Words: **molybdenum carbides; noble metal-like behavior; degree of carburization; density of sites; hydrogenating activity.**

INTRODUCTION

In 1971 Sinfelt and Yates (1) showed that the carburization of molybdenum greatly increases the specific activity of molybdenum for ethane hydrogenolysis. Several other studies since then have shown that molybdenum carbides, along with other carbides and nitrides, are active catalysts in several chemical reactions normally catalyzed by noble metals, as reviewed elsewhere (2–4). In particular, Mo_2C prepared *in situ* without free carbon and oxygen contamination is an excellent catalyst for hydrogenation or hydrogenolysis of hydrocarbons and is comparable to noble metals such as Ru. Why do nitrides or carbides of early transition metals catalyze reactions characteristic of precious metals, in contrast to their parent metals? This question can be first explained qualitatively by the evolution of electron density of states as follows. The introduction of C or N atoms in the lattice of an early transition metal leads to an increase of its lattice parameter a_0. The increase in the metal–metal distance leads to a contraction of the *d*-band (proportional to $1/a_0^5$) (5). Hence the *d*-electron density of states of the early transition metal becomes higher at the Fermi level after carburization or nitridation, conferring to the parent metal an electron density of states similar to that of noble metals. From this elementary theory on carbides or nitrides it can be predicted that the higher the carbon or nitrogen contents, the higher will be the noble metal-like behavior of these materials.

From a practical point of view, molybdenum carbides became all the more interesting after several methods were developed, leading to high specific surface area (S_g) Mo_2C (4). The temperature-programmed reaction (6–10) proposed by the group of Boudart has been frequently adopted by many research groups in catalysis to prepare early transition metal carbides and nitrides with high S_g. The work by Lee *et al.* (9) is a typical example of preparation of bulk Mo_2C by this method. It consists of treating MoO_3 in a flowing mixture of methane in hydrogen (CH_4/H_2) with the temperature increasing slowly in a controlled manner. Starting from low surface area MoO_3, these authors have synthesized hexagonal Mo_2C samples, with S_g ranging from 50 to 100 $m^2\ g^{-1}$, whereas Mo_2C prepared isothermally had only 5 $m^2\ g^{-1}$. Flow rate of gases, CH_4/H_2 ratio, heating rate, final temperature, isothermal duration at this final temperature, and treatment after carburization are important parameters which determine the properties of the resulting Mo_2C

[1] To whom correspondence should be addressed. Fax: (33) 1 44 27 36 26. E-mail: djega@ccr.jussieu.fr.

0021-9517/00 $35.00

(9, 11, 12). Nevertheless, no study has been conducted, to our knowledge, to investigate the completion of carburization and its effects on the noble metal-like catalytic properties of the resulting Mo_2C.

A passivation step has to be done after synthesis of these pyrophoric carbides, to avoid their bulk oxidation when contacting air. Nevertheless, a passivated sample is completely inactive in benzene hydrogenation at room temperature (one of the most difficult reactions to do) (13), whereas an *in situ* prepared Mo_2C is as active as Ru in this reaction (14–16). Therefore, it appears that oxygen causes very strong deactivation in the hydrogenating function of carbides (13).

Another important parameter controlling the activity of carbides is the amount of free carbon deposited on the surface of the solid during its preparation. This free carbon deposit on active sites inhibits the reaction.

The present work was dedicated to the synthesis of bulk Mo_2C presenting a controlled "clean" surface (without free carbon and oxygen contamination) and a high specific surface area for the purpose of its utilization as active catalyst in hydrogenation of hydrocarbons. In particular, the main objective will be to demonstrate experimentally the aforementioned theory on the noble metal-like behavior of Mo_2C: the higher the carbidic carbon content and the lower the residual oxygen content, the higher will be the noble metal-like behavior of the carbide. Both carbidic carbon and residual oxygen contents will define the "degree of carburization." In what follows, we shall see that the degree of carburization will drastically affect the nature of active sites.

Two experimental approaches were carried out to characterize the noble metal-like behavior of Mo_2C according to its degree of carburization. First, the counting of noble metal-like surface Mo sites was realized by selective CO chemisorption. Then, the quantitative evaluation of the "quality" of these sites was done by measuring activity per site for a probe reaction. Benzene hydrogenation was chosen in this study for this purpose.

EXPERIMENTAL

Commercial molybdic acid powder (containing ammonium ions, Fluka) was used as received for the preparation of samples of molybdenum carbides. For each preparation, the precursor was loaded on a coarse quartz fritted disk in a quartz reactor which could be isolated by stopcocks after synthesis and then transferred to chemisorption or benzene hydrogenation units without exposure of the sample to air. As reactant gases, CH_4 (Air Liquide, 99.90%) and H_2 (Air Liquide, 99.995%) were employed. Prior to flowing into the reactor, the mixture (10 or 20 vol% CH_4/H_2) was purified consecutively through a molecular sieve trap, an oxygen trap (Alltech, Oxy-Purge N), and an indicating oxygen trap (Alltech, Indicating Oxy-Purge). The synthesis was realized at atmospheric pressure with a molar hourly space velocity (MHSV) of 68 h^{-1}. The temperature programming was performed by a temperature regulator/controller (Setaram TGC85). A heating rate of 53 K h^{-1} and final temperatures between 923 and 1048 K were used. The reactor was maintained from 0 to 4 h at a given final temperature before being quenched to room temperature (RT). The evolution of gases was monitored by analyzing the effluent gases with a gas chromatograph (IGC 12M Intersmat-DELSI) equipped with a thermal conductivity detector (TCD). The separation of gases was realized on a 0.9-m-long, 3-mm-diameter (o.d.) column packed with Porapak N (Alltech) and then on a 1.8-m-long, 3-mm-diameter (o.d.) column packed with carbon molecular sieves (Carbosieve SII). After synthesis, the reactor was closed and isolated from the atmosphere and transported either to the chemisorption or to the benzene hydrogenation units. When necessary, before exposure to air, the prepared samples were passivated by pulses of oxygen in flowing helium.

Thermogravimetric analysis (TGA) was conducted under conditions similar to those of synthesis in order to investigate the variation of weight during the synthesis. Precursor loading of 0.056 g, total flow rate of 22 μmol s^{-1}, and heating rate of 114 K h^{-1} were employed for the experiment. The apparatus was equipped with a microbalance (Setaram MTB 10-8), a gas delivery system, a furnace, and a temperature regulator/controller (Setaram RT3000).

Elemental analysis of the solids was performed by the Service Central d'Analyse du Centre National de la Recherche Scientifique (Vernaison, France). Amounts of hydrogen, carbon, nitrogen, and oxygen were determined by combustion of the solid and analysis of the effluent gases. Molybdenum analysis was realized by plasma emission spectroscopy.

A Siemens D500 automatic diffractometer with a Cu$K\alpha$ monochromatized radiation source was used for the X-ray diffraction (XRD) powder patterns of various intermediates during the carburization, as well as of the final Mo_2C. The identification of the different solid phases was made using the JCPDS (Joint Committee on Powder Diffraction Standards) library for molybdic acid (ammonium molybdenum hydrogen oxide hydrate) (No. 46-0100), Mo_4O_{11} (No. 5-0337), MoO_2 (No. 32-0671), Mo(No. 42-1120), and Mo_2C (No. 35-0787). The lattice parameters of the hexagonal close-packed molybdenum carbides were determined using a refinement program (17). The average size (D_c) of coherently diffracting domains perpendicular to (*hkl*) planes was evaluated by the Scherrer formula (18) from the half-width of the (*hkl*) X-ray diffraction line corrected for instrumental broadening.

The specific surface areas of the samples were obtained from nitrogen desorption at RT after adsorption of N_2 at different partial pressures (10, 20, and 30 kPa) at 77 K, by means of the BET method (19). Measurements were

performed using a Quantachrom-Quantasorb Jr. dynamic sorption system after pretreatment of the sample in flowing N_2 (41 μmol s^{-1}) (Air Liquide, 99.995%) at 673 K for 1 h. The amounts of N_2 adsorbed at liquid nitrogen temperature and desorbed at RT were determined by using a TCD. The measured specific surface areas were used to calculate the corresponding particle sizes (D_p) from the equation $D_p = 6/(\rho S_g)$, assuming a spherical shape, where ρ is the density of solid.

Pulsed chemisorption technique (20) was employed to measure the amount of irreversibly chemisorbed CO or O_2 on the prepared Mo_2C. Pulses of a known quantity (17 μmol) of CO (Air Liquide, 99.997%) or O_2 (Air Liquide, 99.5%) were injected every 5 min on the sample at RT in flowing He (30 μmol s^{-1}) (Air Liquide, 99.995%) purified by an oxygen trap (Oxysorb, Messer Griesheim). The injection was continued until the surface was saturated by probe molecules. After each injection, the quantity of probe molecules not chemisorbed was measured using a conventional device equipped with a TCD.

Benzene hydrogenation was carried out at RT and atmospheric pressure under dynamic differential conditions. A flow (74 μmol s^{-1}) of H_2 purified as for the synthesis was passed through a benzene (Merck, 99.8%) saturator, then through a condenser maintained at RT and 286 K, respectively. Thus, the initial partial pressures of benzene and hydrogen were 6.9 and 94.4 kPa, respectively. Unreacted benzene and products were analyzed by an on-line gas chromatograph (HP 5890 Series II) equipped with a flame ionization detector and a 50-m-long and 0.2-mm-diameter (i.d.) capillary column (HP PONA, 0.5 μm film thickness). A commercial Ru/Al_2O_3 (Johnson Matthey) was tested as a reference catalyst and compared with the carbides. Before reaction, 5 wt% Ru/Al_2O_3 was reduced *in situ* in flowing H_2 at 723 K for 2 h.

Temperature-programmed reduction (TPR) was performed for Mo_2C samples prepared *in situ*. These results were used to evaluate the degree of carburization of Mo_2C samples. Flowing H_2 (MHSV = 32 h^{-1}) purified as for the synthesis was used and the heating rate was 420 K h^{-1}. The gaseous products (CH_4 and H_2O) evolved during the reaction were analyzed by a gas chromatograph (IGC 12 M Intersmat-DELSI) equipped with a TCD. Gases were separated on a 0.9-m-long and 3-mm-diameter (o.d.) column packed with Porapak N (Alltech).

RESULTS AND DISCUSSION

Carburization

The carburization of molybdic acid, containing ammonium ions, was monitored by analyzing the effluent gases during the reaction. An example of this carburization is shown in Fig. 1a. The reaction was conducted in a flow (62 μmol s^{-1}) of 10 vol% CH_4/H_2 over 0.5 g of molybdic acid, corresponding to 68 h^{-1} of MHSV. The heating rate was 53 K h^{-1}. We can see three peaks for water (400 K, 680 K, and 900 K) and a CH_4 consumption peak. This CH_4 consumption occurs almost simultaneously with the third stage of water production and with the formation of a small peak of CO. In addition, we have another small peak due to traces of N_2 (coming from ammonium ions of the Mo precursor) around 630 K. Traces of NH_3 and CO_2 were also detected during the carburization, but in very small quantities. Thus, these gases are not presented in Fig. 1a. TPR of molybdic acid in flowing pure H_2 is presented in Fig. 1b for the sake of comparison. The TPR conditions were the same as for the synthesis of carbides except for the nature of the flowing gas. Again we observe three peaks of water at almost the same temperatures as for the carburization and one small peak of N_2.

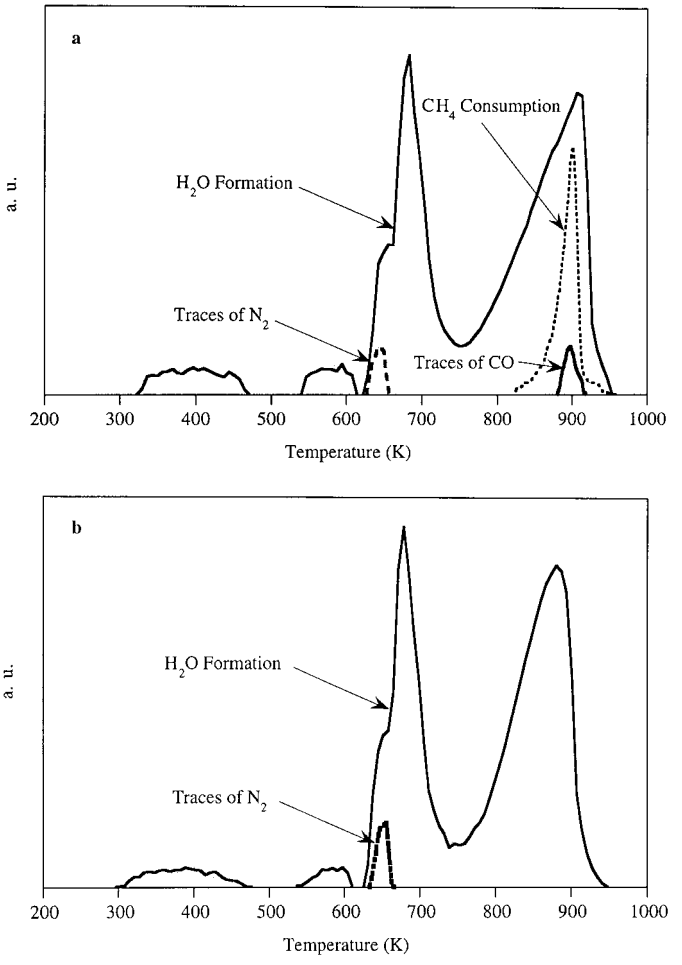

FIG. 1. Temperature-programmed reaction profiles of molybdic acid (a) in flowing 10 vol% CH_4/H_2 and (b) in flowing pure H_2 (precursor loading = 0.5 g, total flow rate = 62 μmol s^{-1}, heating rate = 53 K h^{-1}).

Figure 2 shows the results of TGA realized to investigate the evolution of weight during the TPR synthesis. We observe three significant losses of weight without any well-defined plateau during the synthesis. The arrows in

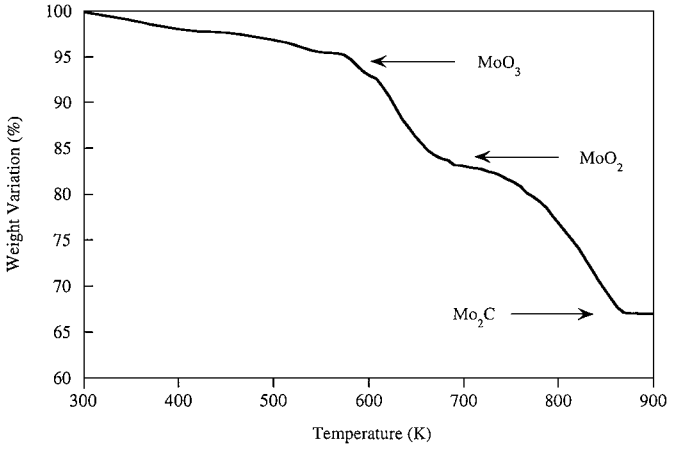

FIG. 2. TGA of the carburization of molybdic acid in flowing 10 vol% CH_4/H_2 (precursor loading = 0.056 g, total flow rate = 22 μmol s^{-1}, heating rate = 114 K h^{-1}). Arrows indicate the theoretical plateaus of weight for MoO_3, MoO_2, and Mo_2C.

the figure indicate the positions of the theoretical plateaus which could be observed if the carburization proceeds through non-concomitant formation of MoO_3 and MoO_2. The temperatures of the three weight losses are in good agreement with those of the three water peaks in Fig. 1a.

To better define the carburization steps, the synthesis intermediates were characterized by XRD. The reactor was quenched during the carburization at given temperatures chosen with the help of the chromatographic and thermogravimetric analyses described above. The intermediates were then passivated before XRD analysis. The resulting diffraction patterns are shown in Fig. 3. The diffraction patterns of the precursor as well as of the resulting Mo_2C are also presented for the sake of comparison. The precursor (the commercial molybdic acid) shows, in fact, a diffraction pattern similar to that of ammonium molybdate corresponding to a body-centered cubic structure (21). This structure is maintained up to 523 K. Therefore, the first peak of water in Fig. 1a and the first weight loss in Fig. 2 can be attributed to the dehydration of the precursor. Above 623 K the structural evolution begins to occur. Indeed, we see a decrease of the initial precursor phase while a nonstoichiometric oxide, Mo_4O_{11}, appears. The diffraction pattern obtained at 733 K is that of pure MoO_2. It explains the second peak of water in Fig. 1a and weight loss in Fig. 2, respectively. MoO_2 has been also identified as an intermediate in the carburization of MoO_3 in flowing 20 vol% CH_4/H_2 by Lee *et al.* (9). We notice also the presence of Mo metal as an intermediate along with MoO_2 in the sample at 875 K. This metallic phase persists in the sample at 903 K with MoO_2 and Mo_2C, the total carburization not being achieved. The third peak of water and simultaneous CH_4 consumption in Fig. 1a is linked to this step of carburization. The third weight loss observed by TGA during the carburization is also related to this step (Fig. 2). In Fig. 1a, we can see that the third water production starts earlier than the CH_4 consumption and the peak is much larger than that of CH_4. This observation justifies the existence of Mo metallic intermediate. Leclercq *et al.* (22) have reported that direct carburization of WO_3 by 20 vol% CH_4/H_2 does not take place, but that the carburization occurs via the reduction of WO_3 to W metal as revealed by *in situ* XRD during their temperature-programmed carburization. Hexagonal Mo_2C was obtained by maintaining the reactor at 923 or 973 K. At the top of Fig. 3, the two diffraction patterns are presented for Mo_2C samples prepared at 923 and 973 K, respectively.

Specific surface areas of the aforementioned samples (precursor, intermediates, and products) were measured by the BET method to monitor the evolution of S_g during the carburization. The results are shown in Fig. 4. The tangible development of S_g begins at 733 K, and then the development of S_g continues until the carburization is finished. Once the carburization is achieved, S_g begins to decrease.

Physical Properties and Difficulty in Evaluating the Completion of the Carburization

Table 1 summarizes the synthesis parameters and some physical properties of the resulting Mo_2C. According to the preparation conditions, S_g varies from 40 to 91 $m^2\,g^{-1}$, showing a sensitive effect of the synthesis parameters on S_g of

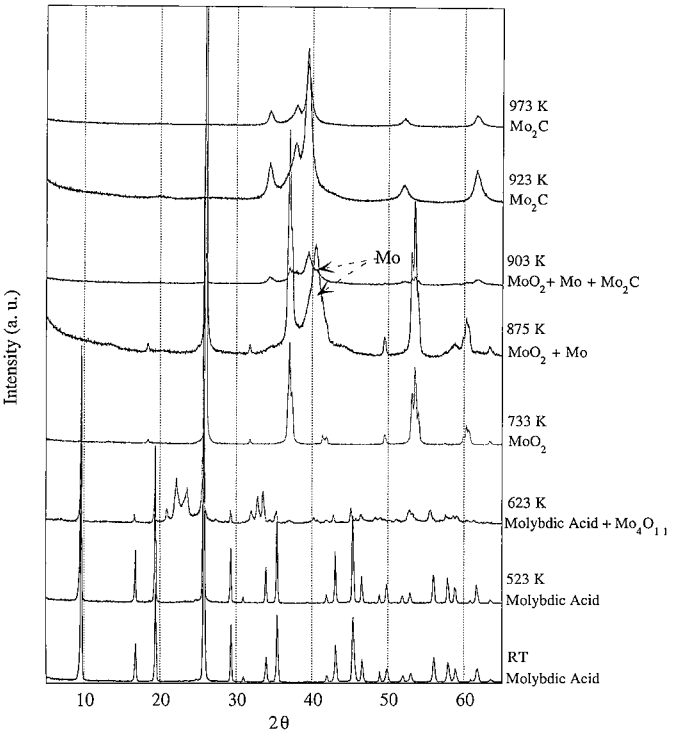

FIG. 3. XRD study of the evolution of the crystallographic structure during the temperature-programmed carburization of molybdic acid in flowing 10 vol% CH_4/H_2. To obtain the two patterns of Mo_2C shown at the top of the figure, the reaction was maintained for 1 h at the final temperature.

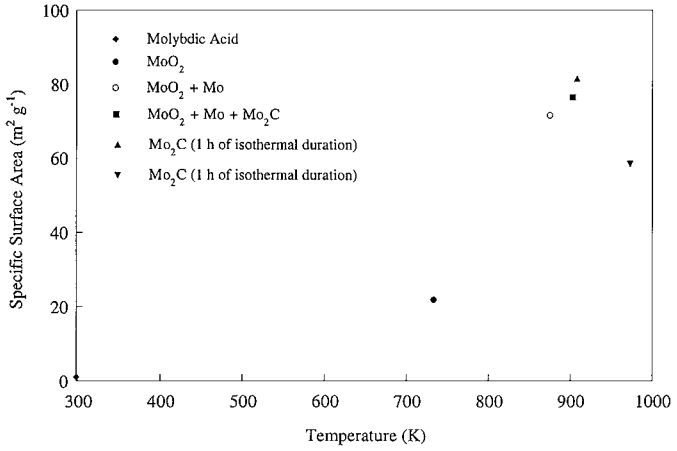

FIG. 4. Evolution of the specific surface area during the temperature-programmed carburization of molybdic acid in flowing 10 vol% CH_4/H_2.

TABLE 2

Elemental Analysis of the Precursor and Mo_2C Samples[a] (Mole per Mole of Mo)

Sample	C	O	N	H
Molybdic acid		2.89	0.18	1.10
10MoC1	0.43			
10MoC2	0.45			
10MoC3b	0.50			
10MoC4	0.48			
20MoC2b	0.50			
20MoC3	0.84			

[a] For Mo_2C samples only Mo and C contents were measured. N content was negligible in these Mo carbides.

the resulting carbides. The higher the concentration of CH_4 was, the higher S_g was at a given final temperature (e.g., 10MoC2 vs 20MoC2b). On the other hand, the increase in the final temperature gave rise to the decrease in S_g for each concentration of CH_4 (e.g., 10MoC1 vs 10MoC2). For the same concentration of CH_4 and temperature of carburization, the longer the isothermal duration was, the smaller S_g was (e.g., 10MoC3a vs 10MoC3d).

As shown previously (Fig. 3), the only crystalline phase observed in the molybdenum carbides was the hexagonal Mo_2C. No significant difference in lattice parameters was observed in these samples as shown in Table 1. In fact, there might be some trend in c_0 parameter with crystallite sizes: a decrease of c_0 is observed with increasing crystallite size. However, considering the reported standard deviations (Table 1), it was difficult to consider this tendency significant. Therefore, we could not estimate the completion of carburization by an evolution of lattice parameters. The crystallite sizes obtained from XRD measurements are in good agreement with the particle sizes determined from BET specific surface areas. This means that the primary particles of Mo_2C are single crystals.

Elemental analysis of the precursor and some prepared Mo_2C samples is presented in Table 2. It shows that the precursor (molybdic acid) contains some amount of nitrogen. In contrast, the N content of Mo_2C samples is negligible in all cases. However, the C content in Mo_2C is quite different from one to another according to the synthesis parameters. For a stoichiometric Mo_2C, the molar ratio C/Mo is 0.5. Table 2 shows that 10MoC3b, 10MoC4, and 20MoC2b, corresponding to different concentrations of CH_4 and temperatures of carburization, are very near

TABLE 1

Synthesis Parameters and Some Physical Properties of Hexagonal Close-Packed Mo_2C Samples

Catalyst code	Synthesis parameters			Lattice parameters[a]		Crystallite size,[b]	Surface area	Particle size,[c]
	CH_4/H_2 (vol%)	Final temperature (K)	Isothermal duration (h)	a_0 (Å)	c_0 (Å)	D_c (Å)	($m^2\ g^{-1}$)	D_p (Å)
10MoC1	10	923	1	3.0106(7)	4.7528(13)	105	84	79
10MoC2	10	973	1	3.0080(9)	4.7446(17)	118	61	108
10MoC3a	10	1023	0	3.0104(12)	4.7463(22)	131	56	118
10MoC3b	10	1023	1	3.0100(6)	4.7450(11)	151	49	135
10MoC3c	10	1023	2	3.0104(15)	4.7439(28)	175	44	150
10MoC3d	10	1023	4	3.0117(7)	4.7433(12)	176	40	165
10MoC4	10	1048	1	3.0103(4)	4.7426(7)	172	43	153
20MoC1	20	923	1	2.9984(36)	4.7594(67)	75	91	72
20MoC2a	20	973	0	3.0061(47)	4.7759(88)	74	77	86
20MoC2b	20	973	1	3.0048(32)	4.7620(87)	78	72	92
20MoC2c	20	973	2	3.0054(8)	4.7614(24)	84	69	96
20MoC3	20	1023	1	3.0095(53)	4.7266(96)	87	63	105

[a] Figures in parentheses show standard deviation.
[b] Determined from XRD measurement.
[c] Determined from BET surface area.

stoichiometric. In contrast, for 10MoC1 and 10MoC2 carburized at lower temperatures, the C/Mo ratios are less than stoichiometric, which can be explained by a limited carburization. The 20MoC3 sample, carburized at 1023 K with a higher CH_4 concentration, clearly shows an excess of carbon due to the deposition of free surface carbon. Nevertheless, the data from CO chemisorption (see below) shows that elemental analysis does not permit a clear evaluation of the completion of carburization. Indeed, even if 10MoC3b and 20MoC2b present the same C/Mo ratio (0.5), they chemisorbed 0.54×10^{15} and 0.48×10^{15} CO molecules cm^{-2}, respectively. This means that they do not present the same surface state. Furthermore, the technical difficulty of transferring samples without contacting air prevented us from quantifying the amount of residual oxygen in these carbides by elemental analysis.

Thus, for a better evaluation of the completion of the carburization process, the chemisorption of a molecular probe is necessary. Oxygen, as shown below, is not adequate, whereas CO has been found to titrate selectively the noble metal-like Mo atoms active in benzene hydrogenation. In what follows, n_{O_2} or n_{CO} represents the number of chemisorbed O_2 or CO molecules per unit surface area of carbide and will be called "density of sites."

Chemisorption of Oxygen and Control of the Presence of Surface Free Carbon

Table 3 reports data on oxygen chemisorption at RT. Column 3 clearly shows that O_2 uptake is proportional to the total surface area of the first three samples, as it has been controlled by repeated measurements. Column 4 shows the constant value of the number of chemisorbed O_2 per square centimeter on these samples. In contrast, for the sample 20MoC3, which is covered with free carbon (C/Mo = 0.84), no more Mo atoms remain practically accessible to O_2 (0.05×10^{15} O_2 molecules cm^{-2}). Assuming a stoichiometry of two oxygen atoms per Mo atom and a theoretical surface density of Mo atoms of $1.0 \times 10^{15}\,cm^{-2}$, the above data show that oxygen (i) is an indiscriminate molecular probe able to titrate all accessible surface Mo atoms and (ii) permits control of the formation of free carbon. Our oxygen chemisorption data (for the first three samples in Table 3) are quite consistent with those obtained by St. Clair *et al.* (23), who reported studies on CO and O_2 chemisorptions on Mo_2C samples. They assumed a stoichiometry of one CO per surface site and two oxygen atoms per surface sites as in our work. An oxygen surface concentration of $0.88 \times 10^{15}\,cm^{-2}$ was reported by the authors for a sample prepared with a final temperature of 961 K, whereas $0.25 \times 10^{15}\,cm^{-2}$ was given for another sample prepared using 981 K as a final temperature of carburization. A 20 vol% CH_4/H_2 mixture was used for both samples. They attributed this significant difference in site density titrated by oxygen to the difference in free carbon deposit on the surface. Indeed, the XPS analysis of their fresh Mo_2C sample with $0.88 \times 10^{15}\,cm^{-2}$ oxygen site density showed a carbon content of 51 mol%, while the sample with n_{O_2} of $0.25 \times 10^{15}\,cm^{-2}$ showed a carbon content of 70 mol%. As a result, they suggested utility of oxygen site density calculation to titrate all exposed surface Mo atoms. Similar oxygen chemisorption data were also reported on tungsten carbides by Ribeiro *et al.* (24) and by Iglesia *et al.* (25). For example, Ribeiro *et al.* (24) reported that their samples chemisorbed approximately 1 monolayer of oxygen whereas CO chemisorption showed much lower uptake than 1 monolayer. In addition, they reported that the density of polymeric carbon on the surface of their tungsten carbides was very low. In contrast, the low value of 0.05×10^{15} O_2 molecules cm^{-2} observed over 20MoC3 (20 vol% CH_4/H_2 at 1023 K) is also consistent with the data from Choi *et al.* (12). In their study, they carburized MoO_3 by flowing 50 vol% CH_4/H_2 or pure CH_4 at 1093 K. The low value of O_2 uptake on their carbides was attributed to the presence at the surface of graphitic carbon and/or oxygen from the synthesis. To our knowledge, our present paper is the first to report a constant value of oxygen uptake per unit area (one monolayer) over Mo_2C samples prepared under different synthesis conditions, and so with different qualities of carburization. This difference in the quality of carburization upon changing synthesis conditions will be clearly evidenced in the following sections.

TABLE 3

Oxygen Chemisorption of Mo_2C Samples

Catalyst code	Surface area ($m^2\,g^{-1}$)	O_2 uptake ($\mu mol\,g^{-1}$)	n_{O_2}[a] ($\times 10^{15}\,cm^{-2}$)
10MoC2	61	824	0.81
10MoC3b	49	670	0.82
20MoC2b	72	958	0.80
20MoC3	63	52	0.05

[a] Density of surface Mo atoms titrated by O_2.

Selective CO Chemisorption for Titration of Noble Metal-like Surface Mo Atoms

In this study, we assumed from previous studies (26–30) that one molecule of carbon monoxide titrates one surface Mo atom. The relative error in the density of sites titrated by CO chemisorption was estimated to be about 5% on the basis of repeated measurements. Comparison between n_{O_2} ($0.80 \times 10^{15}\,cm^{-2}$, Table 3) and n_{CO} ($0.48 \times 10^{15}\,cm^{-2}$, Table 4) for the same sample 20MoC2b clearly shows that CO does not titrate all surface Mo atoms. According to the theory of heterogeneous catalysis by metals and taking into account the above O_2 and CO chemisorption data, we can assume that CO chemisorption is a selective process: CO titrates only those Mo atoms presenting a noble metal-like behavior. In addition, our additional

TABLE 4

CO Chemisorption of Mo_2C Samples

Catalyst code	Surface area ($m^2\ g^{-1}$)	CO uptake ($\mu mol\ g^{-1}$)	n_{CO}[a] ($\times 10^{15}\ cm^{-2}$)	Percentage of active sites (%)[b]
10MoC1	84	345	0.25	25
10MoC2	61	413	0.41	41
10MoC3a	56	415	0.44	44
10MoC3b	49	437	0.54	54
10MoC3c	44	419	0.57	57
10MoC3d	40	384	0.58	58
10MoC4	43	419	0.58	58
20MoC1	91	383	0.25	25
20MoC2a	77	475	0.37	37
20MoC2b	72	573	0.48	48
20MoC2c	69	505	0.44	44
20MoC3	63	32	0.03	3

[a] Density of surface Mo atoms titrated by CO = density of active sites.
[b] $(n_{CO}/1.0 \times 10^{15}\ cm^{-2}) \times 100$.

study showed that a prior and *increasing* poisoning of Mo_2C surface by successive pulses of CO molecules deactivates *progressively* this catalyst in benzene hydrogenation at 298 K: after a CO uptake corresponding to the total CO chemisorption of the sample, the catalyst becomes completely inactive. This demonstrates clearly that CO titrates active sites of Mo_2C in benzene hydrogenation at RT. This difference between n_{CO} and n_{O_2} was also observed by St. Clair *et al.* (23). These authors also reported that the ratio of oxygen uptake to CO uptake was seen to be relatively constant for the two samples studied. However, in what follows, we shall see that changes in this ratio are very sensitive to the synthesis conditions, which are closely connected to the degree of carburization.

Table 4 shows that for two Mo_2C samples prepared either by 10 (10MoC2) or by 20 vol% CH_4/H_2 (20MoC2b), with the same final temperature (973 K) and isothermal duration of carburization (1 h), the numbers of chemisorbed CO molecules are 0.41×10^{15} and $0.48 \times 10^{15}\ cm^{-2}$, respectively. In other words, n_{CO} was slightly increased by using 20 vol% CH_4/H_2 rather than 10 vol% CH_4/H_2. However 20 vol% does not seem to be generally beneficial for CO chemisorption, because an increase in isothermal duration from 1 h to 2 h at 973 K (from 20MoC2b to 20MoC2c) readily decreased n_{CO} from 0.48×10^{15} to $0.44 \times 10^{15}\ cm^{-2}$. This is probably due to the formation of free carbon on the surface. In contrast, a higher final temperature of carburization has a much higher effect on n_{CO}. The samples prepared with the same CH_4 concentration (20 vol%) and the same isothermal duration (1 h)— 20MoC1 at 923 K and 20MoC2b at 973 K—show, for example, 0.25×10^{15} and $0.48 \times 10^{15}\ cm^{-2}$ of n_{CO}, respectively. Nevertheless, a too high temperature leads to a surface carbon deposit which inhibits both O_2 chemisorption as found previously and CO chemisorption: 20MoC3 in Table 4 clearly shows a very low CO chemisorption ($0.03 \times 10^{15}\ cm^{-2}$). A lower CO uptake was also observed by St. Clair *et al.* (23) on a sample prepared with a higher final temperature of carburization compared to a "clean" Mo_2C sample. Finally, for both the same CH_4 concentration and final temperature, the isothermal duration of carburization controls the selective CO chemisorption: with 10 vol% CH_4/H_2 at 1023 K, 10MoC3a (0 h) and 10MoC3d (4 h) show CO uptakes of 0.44×10^{15} and $0.58 \times 10^{15}\ cm^{-2}$, respectively (Table 4).

Degree of Carburization: Origin of the Evolution of the Density of Active Sites

We explained in a preceding section the origin of the evolution of the density of "noble metal-like" sites titrated by CO chemisorption, by the theoretical concept of the enhanced electron density of states at the Fermi level, due to C insertion into the Mo lattice. As the precursor contains a large amount of oxygen, residual oxygen after incomplete carburization seems to play an important role in the reactivity of Mo_2C as it limits C insertion. This explanation can be corroborated experimentally to the "degree of carburization" defined as the carbidic carbon content, compared to that of residual oxygen in Mo_2C prepared *in situ*.

As we already saw, bulk elemental analysis detects changes in the C content with low sensitivity. It only evidences general trend; Tables 1 and 2 show that C content is increasing with final temperature of carburization (T_f), all other parameters being constant:

Sample	T_f (K)	C/Mo (mol/mol)
10MoC1	923	0.43
10MoC2	973	0.45
10MoC3b	1023	0.50

Furthermore, all samples were characterized by the same XRD pattern of hexagonal Mo_2C, which did not permit any significant lattice parameter change to be followed. Nevertheless, traces of CO and a low consumption of methane were generally observed by the end of carburization, suggesting that the carburization was not complete. To confirm the existence of residual oxygen (leading to CO production during carburization), TPR experiments were proceeded *in situ* on the as-prepared carbides. Once the carburization experiment was over, the sample was cooled to room temperature in flowing CH_4/H_2 mixture, then heated in flowing H_2. Differences in residual oxygen content of 10MoC1, 10MoC2, and 10MoC3b, as detected by the formation of H_2O (TPR peaks of water, Fig. 5), are quite obvious. CO was also detected simultaneously with H_2O but in so low a quantity that its contribution to titrating residual oxygen was considered to be negligible with respect to H_2O formation. There was less water evolving from 10MoC1 to 10MoC3b, whereas a higher temperature was required for

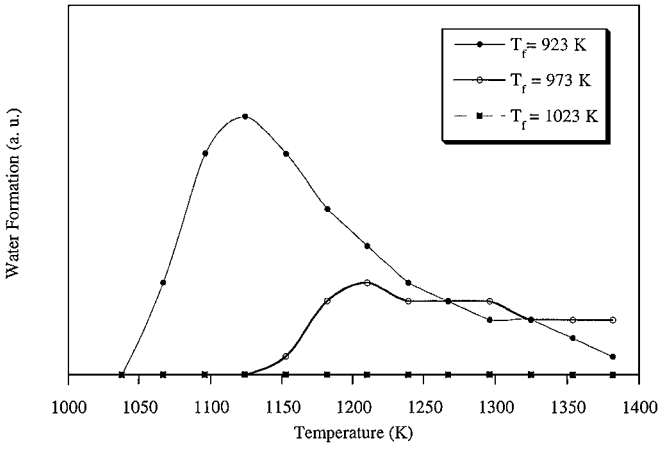

FIG. 5. Water formation during the temperature-programmed reduction of Mo_2C prepared with different final temperatures (T_f). Carburization was done in flowing 10 vol% CH_4/H_2 and with 1 h of isothermal duration.

water to evolve. The lower the residual oxygen content was, the higher was the temperature of its removal with formation of water (Fig. 5):

Sample	T_f (K)	Amount of H_2O	Peak temperature (K)
10MoC1	923	largest	1100–1200
10MoC2	973	60% of 10MoC1	1200–1300
10MoC3b	1023	—	—

Thus, the residual oxygen content of catalysts was

$$10MoC1 > 10MoC2 > 10MoC3b.$$

The final correlation which can be expected in the framework of the model on the behavior of carbides concerns the evolution of n_{CO}: the higher the final temperature of carburization, the lower is the residual oxygen and, if oxygen atoms are replaced by carbon atoms, the higher should be the accessible Mo sites titrated by CO (Tables 1 and 4):

Sample	T_f (K)	n_{CO} ($\times 10^{15}$ cm^{-2})
10MoC1	923	0.25
10MoC2	973	0.41
10MoC3b	1023	0.54

These results are in agreement with those presented previously by Lee *et al.* (9, 31):

T_f (K)	n_{CO} ($\times 10^{15}$ cm^{-2})	Ref.
930	0.22	9
973	0.73	31

In conclusion, oxygen atoms diffuse from the bulk to the surface as carburization proceeds from surface into the bulk. These O atoms can be present near the surface after carburization if the synthesis conditions are not sufficient for the carburization to be complete. It can be expected that residual oxygen removal is simultaneous with carbidic carbon insertion. Thus, the electronic property of the material, as described by the band theory, being a bulk property, we can expect a more pronounced "noble metal-like behavior" of carbides with the degree of carburization. The 10 vol% CH_4/H_2 mixture was found to better control this process, preventing a drastic free carbon deposit as evidenced by oxygen chemisorption. Furthermore, CO appears to titrate Mo atoms active in benzene hydrogenation at 298 K, as long as CO pluses are progressively inhibiting this reaction. These results can explain why the chemisorption of CO was never reported as being close to one monolayer on high surface area molybdenum carbides: carburization was not complete.

Correlation between the Degree of Carburization, the Density of Active Sites, and the Hydrogenating Activity of Mo_2C

Benzene hydrogenation is known for its structure insensitivity (32). Therefore, for all samples of Mo_2C prepared *in situ*, their activity per site should be constant as long as the chemical composition of the active sites remains the same. In contrast if the activity per site differs significantly from one sample to another, it means that the nature of the sites is different in chemical composition. So three samples (10MoC1, 10MoC2, and 10MoC3b) were prepared again in this study to be compared in benzene hydrogenation at RT. These samples showed significant differences in their degree of carburization and density of sites. The activity in benzene hydrogenation was expressed in terms of site time yield (STY). STY is defined as the number of benzene molecules transformed per second per site titrated by CO chemisorption (average turnover rate). The conversion of benzene was maintained below 10% in most cases.

The first remark is that all the samples were active even at RT and comparable to Ru/Al_2O_3, well known as the best catalyst for the reaction (33). Indeed, the highest STY for Mo_2C was ca. 0.09 s^{-1} whereas Ru catalyst showed 0.35 s^{-1}. To calculate the STY of the Ru catalyst, CO chemisorption was done and a stoichiometry of one CO per Ru atom was used. Previously, Lee *et al.* (14, 15) reported Mo_2C/Al_2O_3 was an active catalyst in benzene hydrogenation at 323 K and even more active than Ru catalyst. In the work of Márquez-Alavarez *et al.* (16), Mo_2C has shown a good activity at 373 K in this reaction and its activity was also comparable to that of Ru catalyst. These two groups observed that deactivation occurred during the hydrogenation. As our carbides also showed deactivation, a second-order deactivation law was used to obtain the initial conversion by

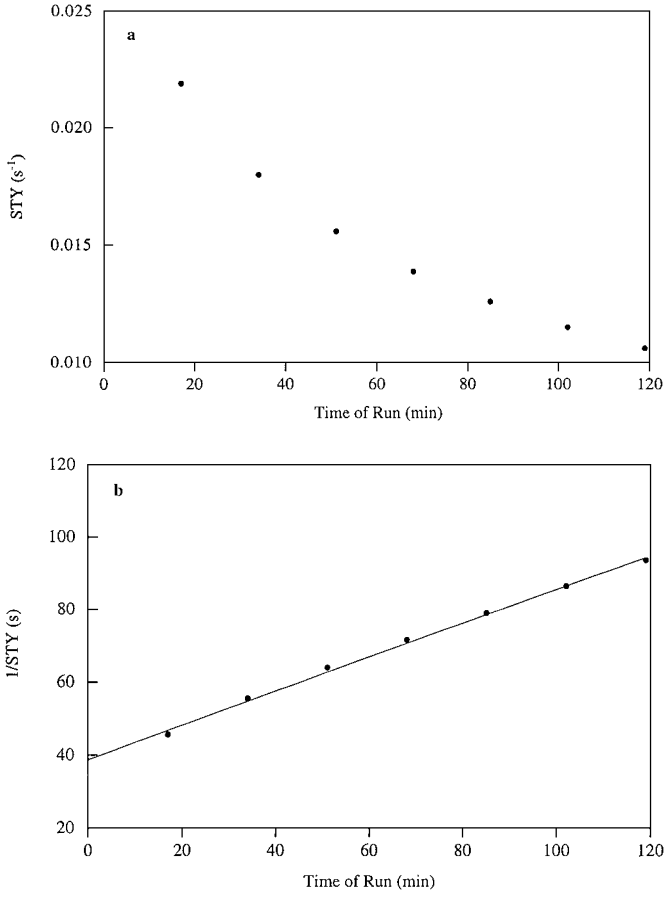

FIG. 6. Variation of benzene hydrogenation activity with time of run for Mo_2C. (a) STY versus time of run. (b) Reciprocal value of STY versus time of run.

extrapolating the deactivation curve to zero time of run (Fig. 6) as discussed elsewhere (34–37).

Figure 7 shows that the activity per site of Mo_2C (STY) increases significantly with the density of sites titrated by CO chemisorption. It means that the degree of carburization influences not only the density of sites, but also the quality of each site (hydrogenating activity). Thus, a clear correlation can be observed between the degree of carburization, the density of active sites, and the hydrogenating activity of Mo_2C. Furthermore, Fig. 7 suggests that the highest STY observed on 10MoC3b was not the maximal activity of the carbide, since the percentage of active sites is still below a monolayer (54%, Table 4). Thus, the degree of carburization can still be improved. Here, the previous work done by Lee *et al.* (14, 15) on Mo_2C supported on Al_2O_3 merits discussion. In their study they observed a much lower activity (STY) on Mo_2C/Al_2O_3 than on Ru/Al_2O_3 when they prepared supported carbides by temperature-programmed carburization of MoO_3/Al_2O_3 in CH_4/H_2 mixture. But when they proceeded to a reduction step in flowing H_2 at a high temperature (1220 K) before carburization with a CH_4/H_2 mixture, their resulting supported carbide showed a much higher activity than that of Ru catalyst. They attributed this difference of activity between the two types of carbides to a possible surface contamination by residual oxygen (15). Our results strongly support this assumption and suggest that direct reduction of oxide precursor at high temperature followed by carburization should lead to a supported Mo_2C with a maximal degree of carburization. But bulk Mo_2C cannot be prepared in this way, as a high-temperature reduction step will lead to a very low surface area. Therefore, selective CO chemisorption and benzene hydrogenation can be useful tools for monitoring the degree of carburization as in our study.

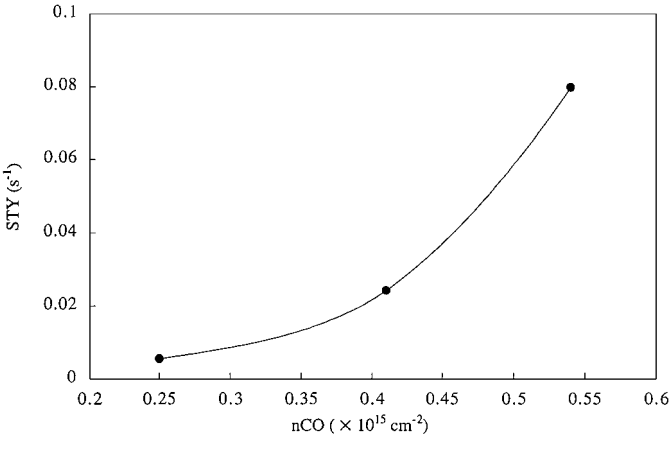

FIG. 7. Correlation between the density of sites (n_{CO}) and the rate of benzene hydrogenation (STY).

CONCLUSION

The important effect of the degree of carburization of molybdenum carbide on its noble metal-like catalytic behavior was evidenced experimentally. Moreover, methods to control the quality of carburization were developed in this study.

Bulk molybdenum carbides were prepared by the temperature-programmed carburization of molybdic acid with CH_4/H_2 mixtures. During the carburization, Mo_4O_{11}, MoO_2, and Mo metal were identified as intermediates by XRD measurements. All samples showed a hexagonal Mo_2C structure and no significant evolution in their lattice parameters was observed with the degree of carburization. The specific surface areas of Mo_2C ranged from 40 to 91 $m^2 g^{-1}$. The particle sizes determined from BET specific surface areas were in good agreement with the crystallite sizes determined from XRD, suggesting that each primary particle is a single crystal. Elemental analysis of the carbides showed different bulk carbon contents according to the preparation conditions. But these results were not sufficiently sensitive to discriminate different "degrees of carburization" of Mo_2C samples.

Two approaches were carried out to evaluate the noble metal-like behavior of Mo_2C. The first one consisted of counting the active sites of the carbides by *in situ* chemisorption measurements. Oxygen was found to titrate all accessible surface Mo atoms, and Mo_2C samples chemisorbed approximately one monolayer of oxygen, if there was no free carbon deposit. Therefore, this probe can be used to control the free carbon formation on the surface of prepared Mo_2C. In contrast, CO was found to inhibit progessively and selectively Mo atoms active in benzene hydrogenation at 298 K. Thus, active-site counting could be done by selective CO chemisorption. The percentage of surface Mo atoms titrated by CO ranged from 3 to 58% of the total surface Mo atoms. TPR in flowing pure H_2 of Mo_2C sample prepared *in situ* showed that this evolution of the density of sites titrated by CO chemisorption is due to the difference in the degree of carburization.

The second approach to evaluate the noble metal-like behavior of Mo_2C was the evaluation of the quality of each site titrated by CO. This evaluation was done by measuring the STY in benzene hydrogenation at RT. All prepared samples were active and comparable to Ru/Al_2O_3, a well-known active catalyst in this reaction. Significant variation of the STY was also observed according to the density of sites determined by CO chemisorption, thus to the synthesis conditions. The higher the density of active sites, the higher was the STY. As benzene hydrogenation is a structure-insensitive reaction, this evolution of activity (per site) was attributed to the difference in chemical composition in the neighboring of surface Mo atoms. Again, the degree of carburization can explain the observed evolution of STY according to the conditions of synthesis.

Despite the formation of bulk hexagonal Mo_2C in all cases, the degrees of carburization of the resulting carbides were quite different according to the synthesis parameters leading to different chemical compositions of the active sites. In conclusion, the degree of carburization influenced not only the number of noble metal-like sites but also the quality of each site. This is in good agreement with a general concept speculated on the noble metal-like behavior of Mo_2C: the higher the carbidic carbon content and the lower the residual oxygen content in the Mo lattice, the higher will be the noble metal-like behavior.

REFERENCES

1. Sinfelt, J. H., and Yates, D. J. C., *Nature Phys. Sci.* **229**, 27 (1971).
2. Oyama, S. T., and Haller, G. L., *in* "Catalysis, Specialist Periodical Reports" (G. C. Bond and G. Webb, Eds.), Vol. 5, p. 333. Royal Chem. Soc., London, 1981.
3. Leclerq, L., *in* "Surface Properties and Catalysis by Non-metals" (J. P. Bonnelle, B. Delmon, and E. Derouane, Eds.), p. 433. Reidel, Dordrecht, 1983.
4. Oyama, S. T., *Catal. Today* **15**, 179 (1992).
5. Heine, V., *Phys. Rev.* **153**, 673 (1967).
6. Volpe, L., Oyama, S. T., and Boudart, M., *Stud. Surf. Sci. Catal. (Preparation of Catalysts III)* **16**, 147 (1983).
7. Volpe, L., and Boudart, M., *J. Solid State Chem.* **59**, 332 (1985).
8. Volpe, L., and Boudart, M., *J. Solid State Chem.* **59**, 348 (1985).
9. Lee, J. S., Oyama, S. T., and Boudart, M., *J. Catal.* **106**, 125 (1987).
10. Lee, J. S., Volpe, L., Ribeiro, F. H., and Boudart, M., *J. Catal.* **112**, 44 (1988).
11. Oyama, S. T., Schlatter, J. C., Metcalfe, J. E., and Lambert, J. M., *Ind. Eng. Chem. Res.* **27**, 1639 (1988).
12. Choi, J.-G., Brenner, J. R., and Thompson, L. T., *J. Catal.* **154**, 33 (1995).
13. Choi, J.-S., Bugli, G., and Djéga-Mariadassou, G., *Stud. Surf. Sci. Catal. (Proceedings of the 12th International Congress on Catalysis, Granada, 2000)*, in press.
14. Lee, J. S., Yeom, M. H., and Lee, D.-S., *J. Mol. Catal.* **62**, L45 (1990).
15. Lee, J. S., Yeom, M. H., Park, K. Y., Nam, I.-S., Chung, J. S., Kim, Y. G., and Moon, S. H., *J. Catal.* **128**, 126 (1991).
16. Márquez-Alavarez, C., Claridge, J. B., York, A. P. E., Sloan, J., and Green, M. L. H., *Stud. Surf. Sci. Catal. (Hydrotreatment and Hydrocracking of Oil Fractions)* **106**, 485 (1997).
17. Williams, D. E., *in* "A Fortran Lattice Constant Refinement Program," LCR-2, USAEC Reports IS-1052. U.S. Government Printing Office, Washington, DC, 1964.
18. Langford, J. I., and Wilson, A. J. C., *J. Appl. Crystallogr.* **11**, 102 (1978).
19. Brunauer, S., Emmett, P. H., and Teller, E., *J. Am. Chem. Soc.* **60**, 309 (1938).
20. Sayag, C., Bugli, G., Havil, P., and Djéga-Mariadassou, G., *J. Catal.* **167**, 372 (1997).
21. Khan, A. J., Tsuji, M., and Abe, M., *Bull. Chem. Soc. Jpn.* **62**, 3457 (1989).
22. Leclercq, G., Kamal, M., Giraudon, J. M., Devassine, P., Feigenbaum, L., Leclercq, L., Frennet, A., Bastin, J. M., Löfberg, A., Decker, S., and Dufour, M., *J. Catal.* **158**, 142 (1996).
23. St. Clair, T. P., Dhandapani, B., and Oyama, S. T., *Catal. Lett.* **58**, 169 (1999).
24. Ribeiro, F. H., Dalla Betta, R. A., Guskey, G. J., and Boudart, M., *Chem. Mater.* **3**, 805 (1991).
25. Iglesia, E., Ribeiro, F. H., Boudart, M., and Baumgartner, J. E., *Catal. Today* **15**, 307 (1992).
26. Ko, E. I., and Madix, R. J., *Surf. Sci.* **109**, 221 (1981).
27. Erickson, J. W., and Estrup, P. J., *Surf. Sci.* **167**, 519 (1986).
28. Lee, J. S., Lee, K. H., and Lee, J. Y., *J. Phys. Chem.* **96**, 362 (1992).
29. Wang, J., Castonguay, M., McBreen, P. H., Ramanathan, S., and Oyama, S. T., *in* "The Chemistry of Transition Metal Carbides and Nitrides" (S. T. Oyama, Ed.), p. 426. Blackie, Glasgow, 1996.
30. Wang, J., Castonguay, M., Deng, J., and McBreen, P. H., *Surf. Sci.* **374**, 197 (1997).
31. Lee, J. S., Song, B. J., Li, S., and Woo, H. C., *in* "The Chemistry of Transition Metal Carbides and Nitrides" (S. T. Oyama, Ed.), p. 398. Blackie, Glasgow, 1996.
32. Aben, P. C., Platteeuw, J. C., and Stouthamer, B., *in* "Proceedings of the 4th International Congress on Catalysis, Moscow, 1968," Vol. 1, p. 395. Akadémiai Kiadó, Budapest, 1971.
33. Kubicka, H., *J. Catal.* **12**, 223 (1968).
34. Germain, J.-E., and Maurel, R., *C. R. Acad. Sci.* **247**, 1854 (1958).
35. Marques Da Cruz, G., Djéga-Mariadassou, G., and Bugli, G., *Appl. Catal.* **17**, 205 (1985).
36. Fajardie, F., Tempère, J.-F., Djéga-Mariadassou, G., and Blanchard, G., *J. Catal.* **163**, 77 (1996).
37. Salin, L., Potvin, C., Tempère, J.-F., Boudart, M., Djéga-Mariadassou, G., and Bart, J.-M., *Ind. Eng. Chem. Res.* **37**, 4531 (1998).